MATH 537 Term Paper: Analysis of a Mathematical Model of Bursting in Dissociated Purkinje Neurons

Niklas Brake

April 12, 2018

Abstract

A common experimental preparation for studying Purkinje cells *in vitro* is via dissociation which seperates the soma from the neurites. These dissociated Purkinje somata are capable of producing spontaneous bursting. Due to the lack of a dendritic arbour, this bursting behaviour must be distinct from the stereotypical dendrite-driven bursting observed in whole Purkinje cells. I have analysed a biophysical Purkinje soma model by Forrest that was designed based on experimental observations of dissociate Purkinje cells. Although the exact results from Forrest's paper could not be reproduced, the model could be modified to reproduce one observation: Persistent Na^+ current is the burst initiator and SK K^+ current is the burst terminator. Importantly, I find that although this modified model also satisfies Forrest's criterion for replicating the experimental observations, the SK and BK currents interact very differently compared to what is presented in Forrest's paper. Thus, I conclude that more work still needs to be done before inference about bursting in dissociated Purkinje cells can be made.

Introduction

Without any synaptic input, *in vitro* Purkinje cells fire in a so-called "trimodal pattern", consisting of tonic spiking, bursting, and quiescence [1]. It has been shown that this bursting behaviour is driven by dendritic calcium spikes [2]. These cells also burst in response to climbing fiber input onto the dendrites, during which the synaptic input induces large calcium transients [3, 4].

Sometimes, Purkinje cells are studied in an experimental condition where the soma is dissociated from the dendritic arbour. Interestingly, some of these dissociated somata spontaneously burst [5]. Thus, there must be a mechanism for bursting localized in the soma. Although whole-cell bursting has been experimentally investigated and mathematically modelled [6], less is known about the bursting behaviour of dissociated Purkinje somata, which lack the dendritic arbour necessary for stereotypical Purkinje cell bursting.

Swensen and Bean investigated this type of Purkinje cell bursting experimentally [7] and found that the bursts are characterized by a large TTX-sensitive sodium current at the beginning of the burst and a build up of SK current concomitant with a decay of the sodium current leading to the end of the burst. However, this analysis was performed on elicited bursts, rather than spontaneous bursts. Therefore, Forrest created a Purkinje soma model to investigate whether these results carry over to spontaneous bursting [8].

In this paper, I analyse Forrest's model (hereafter referred to as the "original model") of bursting in dissociated Purkinje cells. I find that the model as described in the paper fails to produce the results depicted. I then modify the model such that it displays bursting and characterize this bursting behaviour with the same numerical experiments as Forrest. My results cast doubt over whether the details of Forrest's model can provide insight into the physiology of Purkinje cells.

Methods

Numerical simulations were performed with MATLAB [1] (Release 2017b, The MathWorks, Inc.), using the ode15s solver. The model soma is a single cylindrical compartment with a length and diameter of 22 μm. The area-specific membrane capacitance (C_m) is 0.8 μF/cm^2.

Models of the following currents were taken from prior literature and incorporated into the model Purkinje soma: fast, medium, and slow voltage-gated potassium currents; BK- and SK-type calcium-sensitive potassium currents; P- and T-type voltage-gated calcium currents; fast, persistent, and resurgent voltage-gated sodium currents; a hyperpolarization-activated non-specific cation currents (I_H); and a leak current. The current densities were adjusted manually by the author of the original paper [8] to fit the model output to experimental data collected by Swensen and Bean [7]. Specifically, the densities were adjusted so that the currents underlying the initiation and termination of each *spontaneous* burst produced by the model reflected

[1] source code available at github.com/niklasbrake/MATH537

Current Type	Conductance (mS/cm^2)
Fast K^+	41.6
Mid K^+	20.8
Slow K^+	41.6
SK K^+	4
BK K^+	72.8
Fast Na^+	0.1
Persistent Na^+	4
Resurgent Na^+	156
T-type Ca^{2+}	0.1
P-type Ca^{2+}	0.52
I_H	1.04
Leak	0.52

Table 1: Maximal conductances in the model soma.

those underlying the *elicited* bursts seen *in vitro*. The channel conductance densities that produced the best fit are presented in Table 1.

Model Equations

All currents are modelled with Hodgkin-Huxley-type equations except for the resurgent sodium current, which is a Markov state model. The reversal potentials are $E_K = -88$ mV, $E_{Na} = 60$ mV, $E_L = -60$ mV, $E_H = -30$ mV for the potassium, sodium, leak, and hyperpolarization-activate cation current respectively. The reversal potential for the calcium currents is calculated using the Goldman-Hodgkin-Katz equation:

$$E_{ghk}(V) = P_{Ca^{2+}} \frac{V(zF)^2}{RT} \frac{[Ca^{2+}]_i - [Ca^{2+}]_o \cdot \exp(-\frac{zF}{RT}V)}{1 - \exp(-\frac{zF}{RT}V)} \tag{1}$$

Where $[Ca^{2+}]_i = 100$ nM is the internal concentration of calcium, $[Ca^{2+}]_o = 2$ mM is the external concentration of calcium, $T = 295K$ is the temperature, $F = 96,485$ C/mol of electrons is Faraday's constant, $z = 2$ electrons / mol of calcium is the valence charge, $R = 8.631$ J/mol K is the gas constant and $P_{Ca^{2+}} = 2 \times 10^{-5}$cm/s.

The fast-sodium current has a reversal potential of 45 mV and the T-type calcium current has a fixed reversal potential of 135 mV. The model was simulated at $T = 36$ C and all time constants are adjusted with a Q_{10} factor. g_{max} is the maximal channel conductance per unit area as stated in Table 1.

m, h, and z are Hodgkin-Huxley "gating particles", where

$$\frac{dx}{dt} = \frac{x_\infty - x}{\tau_x} \tag{2}$$

for $x = m, h, z$. x_∞ and τ_x are either stated explicitly or defined in terms of α_x and β_x, where

$$x_\infty = \alpha_x/(\alpha_x + \beta_x) \tag{3}$$
$$\tau_x = 1/(\alpha_x + \beta_x) \tag{4}$$

The time constants τ_x have units of milliseconds.

Master Equation

$$\begin{aligned} C_m \frac{dV}{dt} = -(&I_{K_{\text{fast}}} + I_{K_{\text{mid}}} + I_{K_{\text{slow}}} + I_{BK} + I_{SK} \\ &+ I_{Ca_P} + I_{Ca_T} + I_{Na_F} + I_{Na_P} + I_{Na_R} + I_H + I_L) + I_{\text{app}} \end{aligned} \tag{5}$$

Fast voltage-gated potassium current [9]

$$I_{K_{\text{fast}}} = \mathrm{g}_{\max} m^3 h (V - E_K) \tag{6}$$

$$m_\infty = \frac{1}{1 + \exp\left(-\frac{V+24}{15.4}\right)} \tag{7}$$

$$\tau_m = \begin{cases} 0.103 + 14.9 \cdot \exp(0.035V) & V < -35\text{mV} \\ 0.129 + 1000/\left(\exp\left(\frac{V+100.7}{12.9}\right) + \exp\left(-\frac{V-56}{23.1}\right)\right) & V \geq -35\text{mV} \end{cases} \tag{8}$$

$$h_\infty = 0.31 + \frac{1 - 0.31}{1 + \exp\left(\frac{V+5.8}{11.2}\right)} \tag{9}$$

$$\tau_h = \begin{cases} 0.00122 + 1.2 \cdot \exp - \left(\frac{V+56.3}{49.6}\right)^2 & V < 0\text{mV} \\ 1.2 + 2.3 \cdot \exp\left(-0.141V\right) & V \geq 0\text{mV} \end{cases} \tag{10}$$

where the time constants τ_m and τ_h will need to be divided by $3^{\frac{T-22}{10}}$, if temperatures other than 22 C are to be modelled.

Medium voltage-gated potassium current [9]

$$I_{K_{\text{mid}}} = \text{g}_{\max} m^4 (V - E_K) \tag{11}$$

$$m_\infty = \frac{1}{1 + \exp\left(-\frac{V+24}{20.4}\right)} \tag{12}$$

$$\tau_m = \begin{cases} 0.688 + 1000/\left(\exp\left(\frac{V+64.2}{6.5}\right) + \exp\left(-\frac{V-141.5}{34.8}\right)\right) & V < -20\text{mV} \\ 0.16 + 0.8 \cdot \exp(-0.0267V) & V \geq -20\text{mV} \end{cases} \tag{13}$$

where the time constant τ_m is divided by $3^{\frac{T-22}{10}}$.

Slow voltage-gated potassium current [9]

$$I_{K_{\text{slow}}} = \text{g}_{\max} m^4 (V - E_K) \tag{14}$$

$$m_\infty = \frac{1}{1 + \exp\left(-\frac{V+16.5}{18.4}\right)} \tag{15}$$

$$\tau_m = 0.796 + \frac{1000}{\exp\left(\frac{V+73.2}{11.7}\right) + \exp\left(-\frac{V-306.7}{74.2}\right)} \tag{16}$$

where the time constant τ_m is divided by $3^{\frac{T-22}{10}}$.

BK potassium current [9]

$$I_{BK} = \text{g}_{\max} m^3 z^2 h (V - E_K) \tag{17}$$

$$m_\infty = \frac{1}{1 + \exp\left(-\frac{V+28.9}{6.2}\right)} \tag{18}$$

$$\tau_m = 0.505 + \frac{1000}{\exp\left(\frac{V+86.4}{10.1}\right) + \exp\left(-\frac{V-33.3}{10}\right)} \tag{19}$$

$$\tag{20}$$

$$h_\infty = 0.085 + \frac{1 - 0.085}{1 + \exp\left(\frac{V+32}{5.8}\right)} \tag{21}$$

$$\tau_h = 1.9 + \frac{1000}{\exp\left(\frac{V+48.5}{5.2}\right) + \exp\left(-\frac{V-54.2}{12.9}\right)} \tag{22}$$

$$z_\infty = \frac{1}{1 + \frac{0.001}{[Ca^{2+}]_i}} \tag{23}$$

$$\tau_z = 1 \tag{24}$$

where the time constants τ_m, τ_h, and τ_z are divided by $3^{\frac{T-22}{10}}$.

SK potassium current [10]

$$I_{SK} = \mathrm{g}_{\max} z^2 (V - E_K) \tag{25}$$

$$z_\infty = \frac{48 \cdot [Ca^{2+}]_i^2}{48 \cdot [Ca^{2+}]_i^2 + 0.03} \tag{26}$$

$$\tau_z = \frac{1}{48 \cdot [Ca^{2+}]_i^2 + 0.03} \tag{27}$$

P-type calcium current [9]

$$I_{Ca_P} = \mathrm{g}_{\max} m E_{ghk}(V) \tag{28}$$

$$m_\infty = \frac{1}{1 + \exp\left(-\frac{V+19}{5.5}\right)} \tag{29}$$

$$\tau_m = \begin{cases} 0.264 + 128 \cdot \exp(0.103V) & V < -50\mathrm{mV} \\ 0.191 + 3.76 \cdot \exp - \left(\frac{V+41.9}{27.8}\right)^2 & V \geq -50\mathrm{mV} \end{cases} \tag{30}$$

where the time constant τ_m is divided by $3^{\frac{T-22}{10}}$ and $E_{ghk}(V)$ is defined by equation (1).

T-type calcium current [9]

$$I_{Ca_T} = \mathrm{g}_{max} m h (V - 135) \tag{31}$$

$$\alpha_m = \frac{2.6}{1+\exp\left(-\frac{V+21}{8}\right)} \qquad \beta_m = \frac{0.18}{1+\exp\left(\frac{V+40}{4}\right)} \tag{32}$$

$$\alpha_h = \frac{0.0025}{1+\exp\left(\frac{V+40}{8}\right)} \qquad \beta_h = \frac{0.19}{1+\exp\left(-\frac{V+50}{10}\right)} \tag{33}$$

where m_∞, h_∞, τ_m, and τ_h are calculated from equation (3) and τ_m, and τ_h are divided by $3^{\frac{T-37}{10}}$.

Fast sodium current [9]

$$I_{Na_F} = \mathrm{g}_{max} m^3 h (V - 45) \tag{34}$$

$$\alpha_m = \frac{35}{0+\exp\left(-\frac{V+5}{10}\right)} \qquad \beta_m = \frac{7}{0+\exp\left(\frac{V+65}{20}\right)} \tag{35}$$

$$\alpha_h = \frac{0.225}{1+\exp\left(\frac{V+80}{10}\right)} \qquad \beta_h = \frac{7.5}{0+\exp\left(-\frac{V-3}{18}\right)} \tag{36}$$

where m_∞, h_∞, τ_m, and τ_h are calculated from equation (3) and τ_m, and τ_h are divided by $3^{\frac{T-37}{10}}$.

Persistent sodium current [11]

$$I_{Na_P} = \mathrm{g}_{\max} m (V - E_{Na}) \tag{37}$$

$$\alpha_m = \frac{0.091(V+42)}{1-\exp\left(-\frac{V+42}{5}\right)} \qquad \beta_m = \frac{-0.062(V+42)}{1-\exp\left(\frac{V+42}{5}\right)} \tag{38}$$

$$m_\infty = \frac{1}{1+\exp\left(-\frac{V+42}{5}\right)} \qquad \tau_m = \frac{5}{\alpha_m + \beta_m} \tag{39}$$

where the time constant τ_m is divided by $3^{\frac{T-30}{10}}$

Resurgent sodium current [12]

$$I_{Na_R} = \mathrm{g}_{\max} O (V - V_{Na}) \tag{40}$$

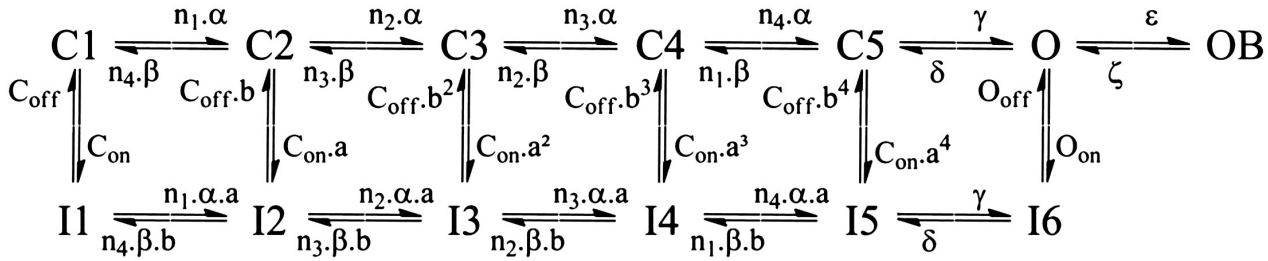

Figure 1: C1-C6 represented 6 closed-state configurations of the channel. O represents the open state, OB the blocked state and I1-I6 the inactivated states. The rate constants are defined in text.

where O is the occupancy of the Open state. The system is described by the Markov model shown in Figure 1.

$$\alpha = 150 \cdot \exp(V/20) \qquad \beta = 3 \cdot \exp(-V/20)$$
$$\gamma = 150 \qquad \delta = 40$$
$$\epsilon = 1.75 \qquad \zeta = 0.03 \cdot \exp(-V/25)$$

$$C_{on} = 0.005 \qquad C_{off} = 0.5$$
$$O_{on} = 0.75 \qquad O_{off} = 0.005$$
$$A = (O_{on}/C_{on})^{1/4} \qquad B = (O_{off}/C_{off})^{1/4}$$

$$n1 = 4 \qquad n2 = 3$$
$$n3 = 2 \qquad n4 = 1$$

The rate constants are all in ms^{-1} and are multiplied by $3^{\frac{T-22}{10}}$.

Hyperpolarization-activated cation current [9]

$$I_H = \mathrm{g}_{\max} m (V - E_H) \tag{41}$$

$$m_\infty = \frac{1}{1 + \exp\left(\frac{V+90.1}{9.9}\right)} \tag{42}$$

$$\tau_m = 0.19 + 0.72 \cdot \exp - \left(\frac{V + 81.5}{11.9}\right)^2 \tag{43}$$

where the time constant τ_m is divided by $3^{\frac{T-22}{10}}$.

Leak current [9]

$$I_L = \bar{g}_{\max}(V - E_L) \tag{44}$$

Intracellular Ca^{2+} Concentration [9] [2]

$$\frac{d([Ca^{2+}]_i)}{dt} = \frac{-10^4 I_{Ca^{2+}}}{zFd} - \beta \cdot [Ca^{2+}]_i \tag{45}$$

where $I_{Ca^{2+}}$ is the calcium current in mA/cm^2, F is the Faraday constant as in equation (1), $d = 0.1$ μm is the depth of the shell, $\beta = 1$ ms^{-1} is the rate of calcium diffusing into the bulk cytoplasm. $[Ca^{2+}]_i$ was constrained by code of the following form:

```
if(Cai<100e-6) Cai = 100e-6;
```

Results

A modified model produces bursting

In the methods sections above, the channel and calcium handling models from the cited literature are reproduced. However these differ from the equations presented in the original paper [8]. Without having access to the model's source code, teasing apart transcription errors in the paper from actual mistakes in the model was a major challenge of reproducing the paper's results.

Although the model in the absence of the persistent Na^+ and SK Ca^{2+}-gated K^+ current does tonically fire as expected, it did not produce bursting upon the addition of these currents as described in the original paper (Fig. 2, A and B). There are two possible reasons for this. The first possibility is that there is some error in the added current models. This is plausible because neither model's equations are accurately presented in the original paper. Indeed, whereas the SK current from [10] is second-order in all calcium concentrations, the model as printed in the original paper is

$$z_\infty = \frac{48 \cdot [Ca^{2+}]_i^2}{48 \cdot [Ca^{2+}]_i^2 + 0.03} \qquad \tau_z = \frac{1}{48 \cdot [Ca^{2+}]_i + 0.03}$$

where notably the calcium concentration in the time constant is of first order. Furthermore, whereas the persistent Na^+ current from [11] is as

[2] Taken from Akemann, Knopfel 2006 on senselab.med.yale.edu/ModelDB/

stated above, the model as cited in the original paper is

$$\alpha_m = \frac{0.091(V+42)}{1-\exp\left(-\frac{V+42}{5}\right)} \qquad \beta_m = \frac{-0.062(V+42)}{1-\exp\left(-\frac{V+42}{5}\right)}$$

where notably, both exponentials are decreasing functions of the voltage. Neither one, nor the other, nor both modifications allowed the model to reproduce the behaviour as depicted in the original paper (Fig. 2, C-E).

The second possibility is that there is some error in the underlying Purkinje cell model, that is, the model without the added persistent sodium and SK current. This is also possible because the original paper contains some important mistakes in the equations concerning calcium dynamics.

Firstly, in the calcium-sensitive potassium current models, the calcium concentration is assumed to be mM. However, in the original GHK equation (1), the calcium concentration is assumed to be in nM. For mM concentrations of calcium, $P_{Ca^{2+}}$ should be given in m/s, but the constant stated in the original paper is in cm/s, thus it is off by a factor of 100. Furthermore, the internal calcium concentration in the equation was fixed at 100 nM despite the model having a dynamic shell-calcium concentration. Finally, the temperature should be 309 K if the simulation is at 36 C, not 295 K.

Secondly, the shell-calcium dynamics stated in the original paper follow the differential equation

$$\frac{d([Ca^{2+}]_i)}{dt} = \frac{-100 I_{Ca^{2+}}}{zFdA} - \beta \cdot [Ca^{2+}]_i$$

where A is the surface area of the cell. However, since the conductances of the calcium channels in the original paper are given in mS/cm^2, the calcium current in this equation is in μA/cm^2, and not nA. Therefore, the normalization to area in the first term is redundant and the scaling is incorrect. Furthermore, the surface area stated in the original paper is 1,521 μm^2. This is correct only if the cell is modelled as an open cylinder. A closed cylinder with the given dimensions would have a surface area of 2,280 μm^2. Thus, several confusions arise from the calcium handling equation in the original paper.

Instead of attempting to reverse engineer the model used by the original investigator, the underlying Purkinje soma model was kept consistent with the prior literature while only the SK and persistent sodium currents were altered. This model was then analysed in parallel with the original paper. Thus, the following alterations to the source literature -derived models were performed:

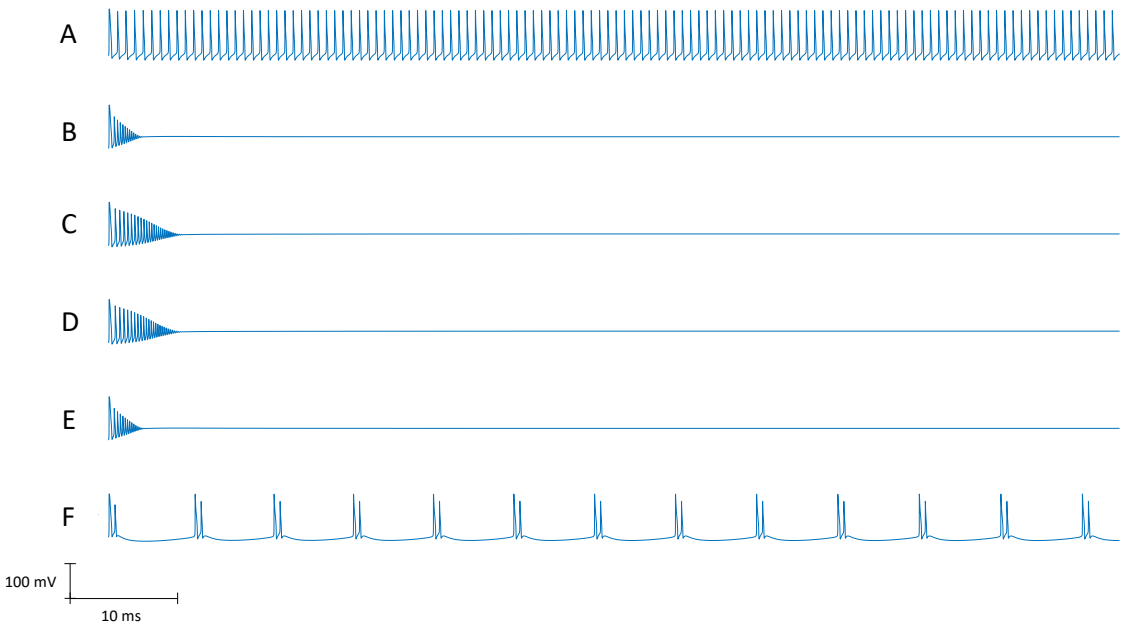

Figure 2: (A) The underlying Purkinje soma model tonically spikes. (B) Upon the addition of I_{SK} and I_{Na_P} with maximal conductances of 4 mS/cm^2, the model converges on an elevated steady state. (C) By incorporating both models as printed in the original text [8], the model does not display bursting. When only I_{Na_P} model is taken from the original text (D) or when only the I_{SK} model is taken from the original text (E), the soma model does not display bursting. (F) When the I_{SK} model is modified as described in equation (46), the model displays bursting with two spikes per burst.

$$I_{SK} = \mathrm{g}_{\max} z^2 (V - E_K)$$

$$z_\infty = \frac{48 \cdot [Ca^{2+}]_i}{48 \cdot [Ca^{2+}]_i^2 + 0.2} \qquad \tau_z = \frac{1}{48 \cdot [Ca^{2+}]_i + 0.3} \tag{46}$$

The first thing to note is that this model is not strictly physiological, as the range of the gating particle is no longer $[0, 1]$. I made this modification while trying to understand what different errors in the SK channel model would have on the excitability of the model. Since this modification allowed bursting (Fig. 2 F), and since thus far I had reason to believe Forrest's model contained errors, I decided to analyse this modified model. It is conceivable

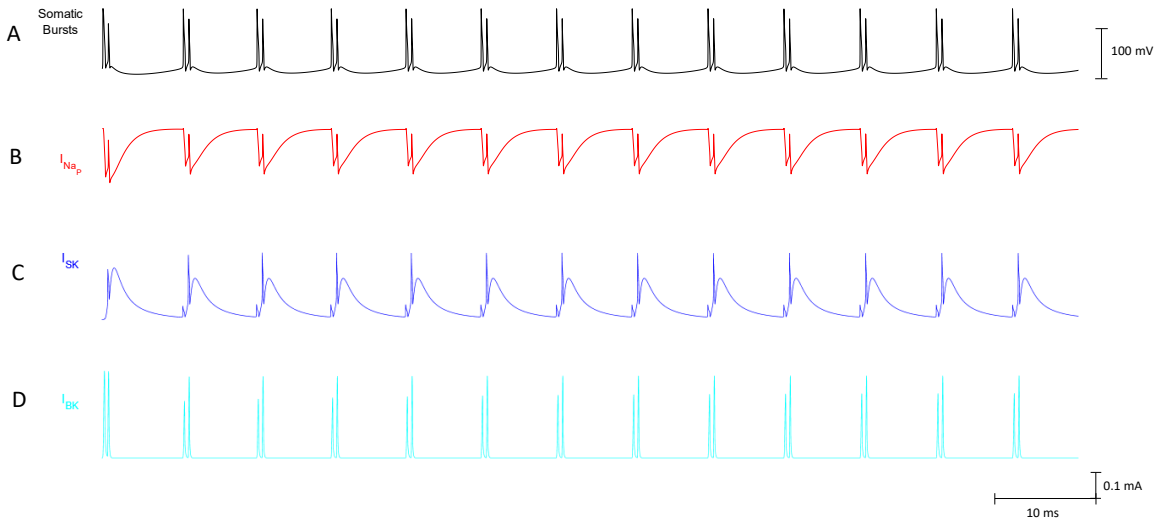

Figure 3: (A) The modelled somatically-driven bursts do not show and change in firing rate, spike height, or a wave of depolarization towards the end as dendritically-driven bursts do. (B) The persistent sodium current does not return to base line in between spikes and builds during the burst. (C) The SK potassium current increases throughout the burst and resets in the inter-burst interval. (D) Similar to the original results [8], the BK current does not increase in magnitude except for the first to second spike. However, this does not occur during the first burst, so the BK current is not responsible for burst termination.

there exists a physiological model equivalent to this modified model given an appropriate scaling of the channel conductance and time constant.

Persistent sodium is the burst initiator and SK potassium is the burst terminator

Having confirmed that adding the Persistent Na^+ current and the SK Ca^{2+}-gated current can switch the Purkinje soma model from spiking to bursting, I next wanted to see the currents underlying the bursting behaviour.

Consistent with what was seen in the original paper, the Persistent Na^+ current (I_{Na_P}) produces a sustained depolarization during the burst that initiates and maintains it (Fig. 3, B). The hyperpolarizing Ca^{2+}-gated K^+ current (I_{SK}) builds during the burst until it attains a high enough magnitude to terminate the burst (Fig. 3, C). Thus, similar to the original model

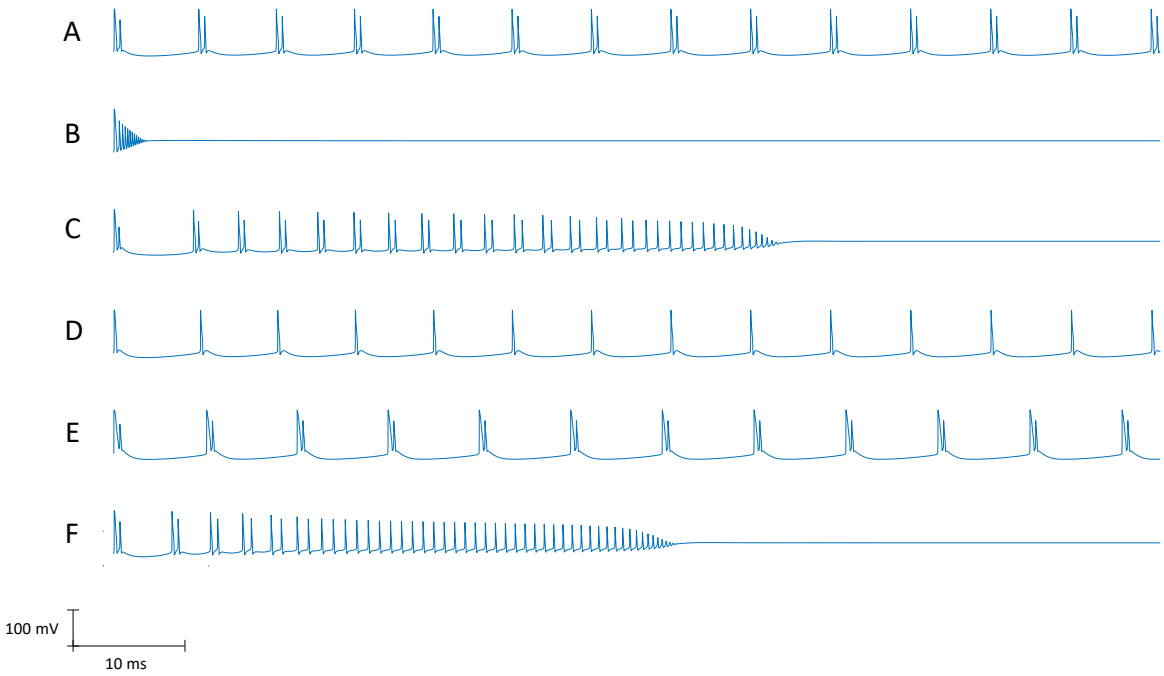

Figure 4: (A) Somatically-driven bursts. (B) $g_{SK} = 0$. The model convergence onto an elevated stable steady state. (C) g_{Na_p} is raised to 7 mS/cm^2. The bursts degrade into spikes and again returns to a silent state. (D) g_{SK} is raised to 8 mS/cm^2. The number of spikes per burst decrease from 2 to 1. (E) g_{Na_P} is raised to 1 S/cm^2. The number of spikes per burst does not change. (F) g_{Ca_T} is increased to 60 mS/cm^2. The model behaves in a similar way as to (C).

[8], this bursting has a "[I_{Na_P} vs. I_{SK}] basis".

Experimental observations of *elicited* somatic bursting indicate that during elicited bursts, the SK current increases progressively during the burst whereas the BK current decreases [7]. My modified model, like the original model, replicates the rising SK current (Fig. 3, C and D). The original model has an increase in BK current between the first and second spike, but then this current decreased over the subsequent two spikes. I did not observe this as my bursts only contain two spikes.

Characteristics of bursting in the Purkinje soma model

Forrest makes eight observations about the bursting characteristics of his model.

1. **I_{Na_P} is not sufficient for bursting; I_{SK} is also required.** If the SK current is removed, the model does not burst. It displays damped oscillations until the voltage converges on an elevated steady state, or as the author calls it, the "depolarization blocked" state (Fig. 4, B).

2. **Increasing the density of I_{Na_P} failed to increase the number of spikes.** In the original model, increasing the density from 4 to 5 mS/cm^2 increased the number of spikes from 4 to 7. This result could not be reproduced. In fact, by raising the density to 7 mS/cm^2, the model demonstrates a sort of damped oscillation, shifting from bursting, to spiking, to an elevated steady state (Fig. 4, C).

3. **Increasing the density of I_{SK} decreases the number of spikes.** This result was reproduced. By increasing the density of I_{SK} from 4 mS/cm^2 to 8 mS/cm^2, the number of spikes per burst decreased from 2 to 1 (Fig. 4, D).

4. **Increasing the density of I_{Na_R} failed to increase the number of spikes.** In the original model, increasing the density from 156 to 300 mS/cm^2 increased the number of spikes per burst from 4 to 7. This result could not be reproduced, even when the density was increased to 1000 mS/cm^2 (Fig. 4, E).

5. **Increasing the density of T-type Ca^{2+} current (I_{Ca_T}) failed to increase the number of spikes.** In the original model, increasing the density from 0.1 to 1 mS/cm^2 increased the number of spikes per burst from 4 to 5. This result could not be reproduced. The bursting behaviour did not seem to change, until the density was raised sufficiently high, which had the same effect as raising I_{Na_P} (Fig. 4, F).

6. **Increasing the density of I_{SK} can switch the model into simple spiking.** This result was reproduced. By increasing the density of I_{SK} from 4 to 20 mS/cm^2, the model switched to simple spiking (Fig. 5, A).

7. **Increasing the density of I_{BK} can switch the model into simple spiking.** This result was reproduced. Whereas the original paper increased the density from 72.8 to 10,000 mS/cm^2, my model was

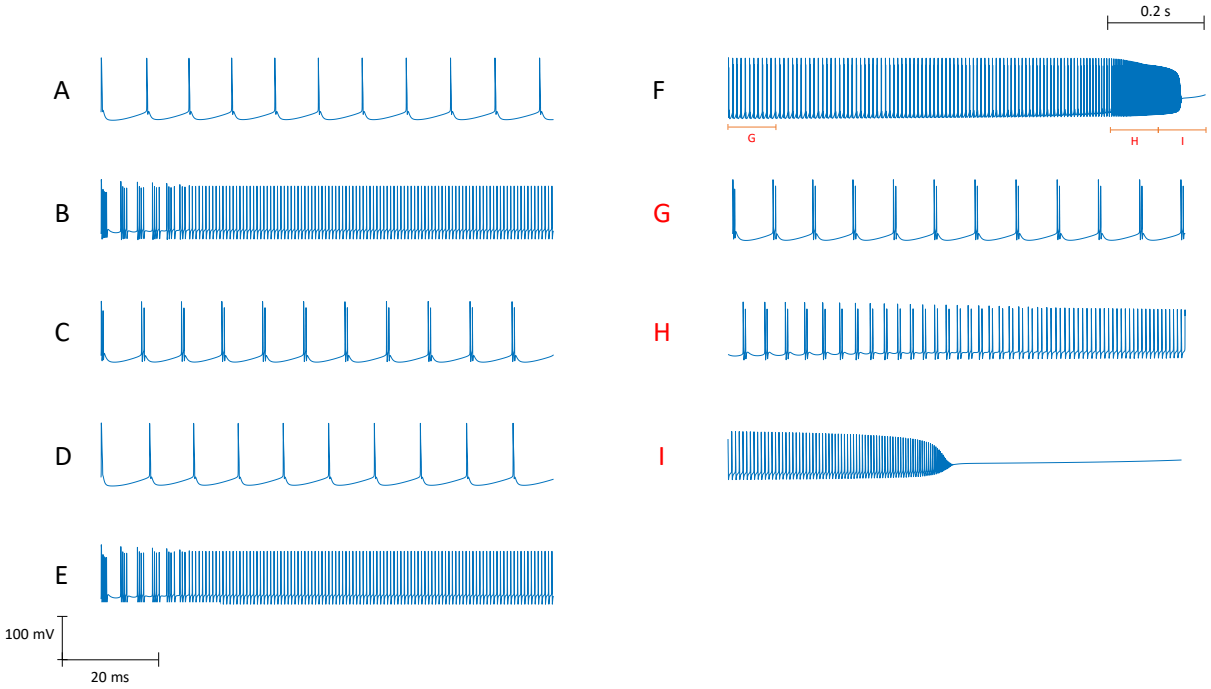

Figure 5: (A) $g_{SK} = 20$ mS/cm^2 produces simple spiking. (B) $g_{BK} = 2$ S/cm^2 produces simple spiking. When both (A) and (B) are implemented together, the model produces bursting. (D) When $g_{SK} = 20$ mS/cm^2 and $g_{BK} = 0$, the model produces spiking. (E) When $g_{BK} = 2$ S/cm^2 and $g_{SK} = 0$, the model produces spiking. (F) When both SK and BK max conductance was decreased linearly from their values in (C) to 0, the model goes from bursting, to spiking, and then to quiescence. (G-I) are close ups of the indicated regions in (F).

already spiking at a very high frequency with an I_{BK} density of 2000 mS/cm^2 (Fig. 5, B).

8. **Increasing the density of both I_{SK} and I_{BK} can switch the model into simple spiking.** In the original model, employing the previous two regimes simultaneously produced simple spiking behaviour. Interestingly, in my modified model, increasing both current densities actually produced bursting again (Fig. 5, C). Therefore, my currents do not seem to be redundantly preventing bursting as seen in the original model. Removing I_{BK} does not lead to bursting because I_{SK} is still blocking it (Fig. 5, D). Removing I_{SK} does not lead to bursting because the I_{BK} block is present (Fig. 5, E). This indicates more complex

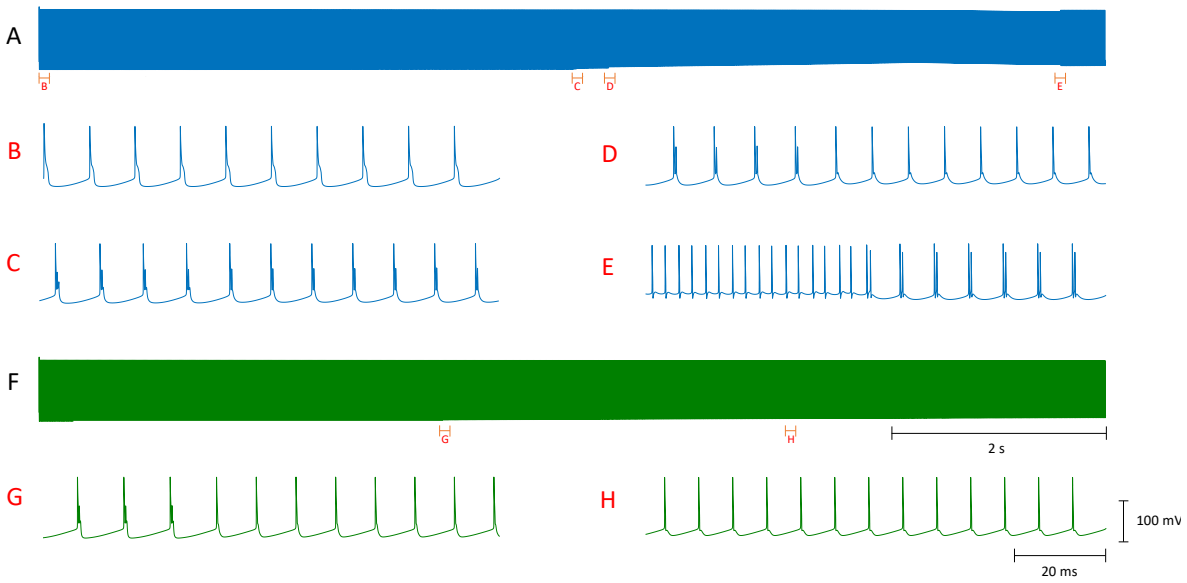

Figure 6: (A) By deceasing the conductance of I_{Ca_P} from 10 to 0 mS/cm^2 over 10s, the model transitions from spiking (B), to bursting (C), back to spiking (D), and finally back to bursting. (F) If the I_{Na_P} conductance is set to zero and the I_{Ca_P} conductance is reduced as in (A), the model goes from the initial high-I_{Ca_P}-bursting to spiking (G-H).

interaction between the two currents than in the original model.

The original paper concludes that "bursting occurs when the depolarization capacity exceeds the repolarization capacity." However this last point demonstrates that bursting can be more complicated than this, as adding more repolarizing capacity (both I_{SK} and I_{BK}) actually rescues the bursting behaviour.

I_{Ca_P} controls the balance between bursting and spiking

If P-type voltage-gated calcium channels are pharmacologically blocked in an intact Purkinje cell, the typical trimodal firing pattern is replaced by a period of bursting activity and then a "depolarization block" [13, 1]. The author of the original paper hypothesized that this is due to blocking I_{SK} and I_{BK}, as they are both calcium-activated. To simulate a gradual block of calcium channels, both current densities were linearly decreasing from their

elevated state to 0 mS/cm^2. This caused the Purkinje cell model to shift from bursting to silence (Fig. 5, F-I), similar to what is seen in the original model. However, the consequences of doing the same to the I_{Ca_P} density is more complicated. Even when the density is 0, the model still bursts, unlike the original model (Fig. 6, A). As the density decreases, the model goes from spiking, to bursting, back to spiking, and finally returns to bursting (Fig. 6, B-E).

The investigators noted that this block can only induce somatic bursting if the "foundations" are present. This was not replicated with my model: if the I_{Na_P} density is set to zero, the model bursts when I_{Ca_P} is high and spikes when I_{Ca_P} is low (Fig. 6, F-H).

The Purkinje soma model can replicate elicited bursting

The experimental data from Swensen and Bean [7] was obtained using a current pulse injection protocol. They would isolate a cell that spontaneously fires simple spikes, silence it with a hyperpolarizing current injection, and then inject a 1 ms depolarizing current to drive the cell to fire. The model developed by Forrest was designed based on the experimental results from this protocol. This model fires bursts spontaneously, however an important question is whether the model can replicate the elicited burst results. Simulating this protocol numerically reveals that it can (Fig. 7). Forrest claims it is therefore possible that this model can provide insight into the mechanism underlying spontaneous bursting.

Discussion

There are several assumption underlying Forrest's model. Firstly, it is assumed that a dissociated cell can be modelled as a closed system. That is, despite the dendritic arbour being removed, the inside of the cell can still be modelled as electrically-distinct from the extra-cellular space. Since disassociated cells clearly display electrical activity [7], there must still be two distinct electrical environments interacting. Therefore, this assumption is probably valid. A second assumption is that the ion currents that the investigator adds to the Purkinje cell model are relevant despite them being based on experimental data collected from granule cells (Na_P) [11] and thalamic reticular neurons (SK) [10]. It's possible that the currents in Purkinje cells follow different dynamics. However, given that currents are generated by conserved families of ion channels, it is probable that the channels underlying these currents are the same channels present in Purkinje cells.

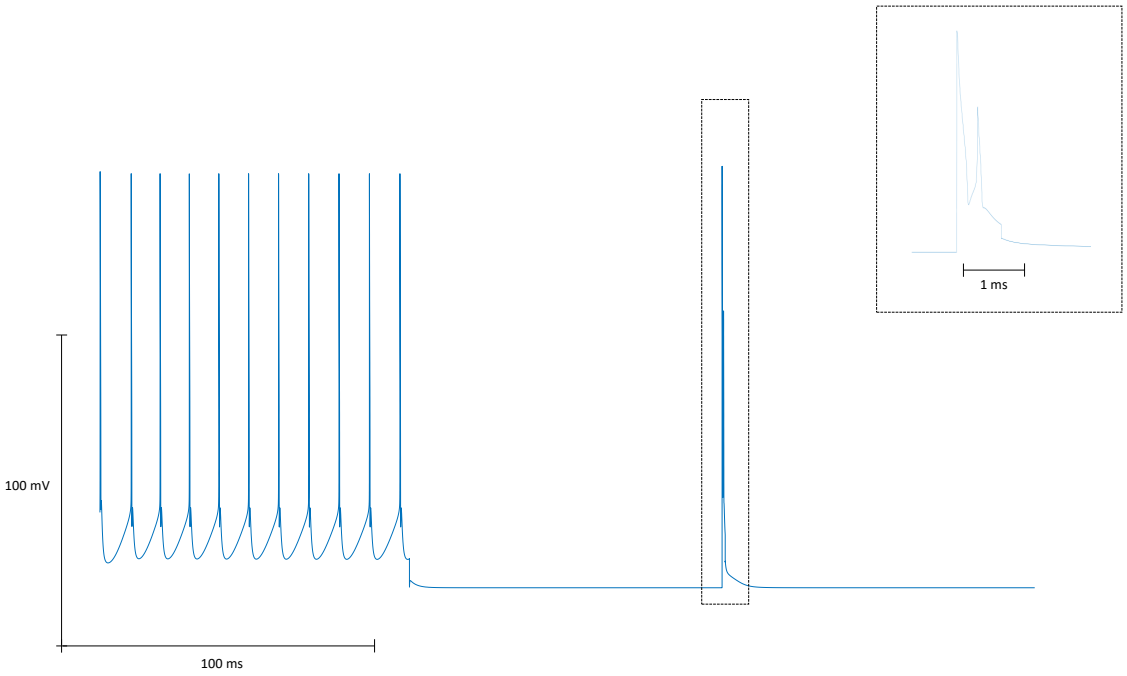

Figure 7: At $t = 100$ ms a hyperpolarizing current of -0.1 mA is injected until $t = 200$, where a 1 ms 0.5 mA depolarizing current. The elicited burst is shown at a higher resolution in the dashed box.

Another important assumption is that not all ion channels of the same species feel the same reversal potential. In Forrest's model, the fast sodium current does not share the same reversal potential as the other sodium currents. Similarly, the T-type calcium current does not have the same reversal potential as the P-type calcium current. Furthermore, the T-type reversal potential is static, despite the calcium concentration near the inside surface of the cell membrane fluctuating by at least an order of magnitude. No explanation is given for this in the original paper. This is troubling, especially in the latter case, because the main conclusion of the paper is that specifically I_{Ca_P} regulates the bursting pattern of the Purkinje soma. Without having a properly dynamic I_{Ca_T}, it is doubtful that the model can provide deep insight into the individual role of I_{Ca_P}. Furthermore, it is stated that the calcium for activating the BK and SK currents is "provided solely by I_{Ca_P} flow in Purkinje cell." However, in the model, both I_{Ca_P} and I_{Ca_T} lead to changes in the internal calcium concentration and this is the signal that

the calcium-activated potassium currents read.

Finally, the assumption on which this paper is constructed is that this model based on data from elicited bursts can give insight into the mechanisms underlying spontaneous bursts. The evidence presented for this assumption being valid is that, by altering the model such that it spikes and performing the same current injection protocol as Swensen and Bean [7], the model displays a qualitatively similar elicited burst. However, my modified model also produces such an elicited burst (Fig. 7), despite the fact that several characteristics of the modified model differ. In particular, increasing the maximal conductance of both the SK and BK current rescued bursting (Fig. 5, C).

Such a discrepancy likely arises due to that fact that no quantitative comparison of the bursts is performed, so the meaning of the burst being "replicated" is ambiguous. Given that the modifications I made to the model are probably physiologically impossible, the modified model does not give insight into the physiology of Purkinje cell bursting. However, Forrest claims that his model does. This claim cannot be justified by a criterion which fails to differentiate between our two models. Moreover, to switch his model from bursting to spiking, Forrest increased the conductance of the BK current by three orders of magnitude without discussing how such a change may be physiological.

In the future, it would be beneficial to construct a Purkinje cell model that bursts with dendritic-driven type bursting and which bursts with somatic-driven type bursting when the dendrite compartments are removed. This would allow better comparisons to the physiological system, as currently it is unknown whether the Forrest's somatic-driven bursting in is compatible with dendritic bursting. Furthermore, developing a quantitative method for measuring "closeness" between a model's output and the experimental data would strengthen the interpretability of the model's validity and make it easier to tune, possibly using cost-function optimization algorithms.

References

[1] Mary D. Womack and Kamran Khodakhah. Dendritic control of spontaneous bursting in cerebellar purkinje cells. *Journal of Neuroscience*, 24(14):3511–3521, 2004.

[2] Mary D. Womack, Carolyn Chevez, and Kamran Khodakhah. Calcium-activated potassium channels are selectively coupled to p/q-type cal-

cium channels in cerebellar purkinje neurons. *Journal of Neuroscience*, 24(40):8818–8822, 2004.

[3] R Llinás and M Sugimori. Electrophysiological properties of in vitro Purkinje cell dendrites in mammalian cerebellar slices. *The Journal of physiology*, 305:197–213, 1980.

[4] H. Miyakawa, V. Lev-Ram, N. Lasser-Ross, and W. N. Ross. Calcium transients evoked by climbing fiber and parallel fiber synaptic inputs in guinea pig cerebellar purkinje neurons. *Journal of Neurophysiology*, 68(4):1178–1189, 1992. PMID: 1359027.

[5] D. L. Gruol and C. L. Franklin. Morphological and Physiological in Cultures of Rat Cerebellum Differentiation of Purkinje Neurons. *The Journal of neuroscience*, 7(May):1271–1293, 1987.

[6] Stefano Masoli, Sergio Solinas, and Egidio D'Angelo. Action potential processing in a detailed Purkinje cell model reveals a critical role for axonal compartmentalization. *Frontiers in Cellular Neuroscience*, 9(February):1–22, 2015.

[7] Andrew M Swensen and Bruce P Bean. Ionic mechanisms of burst firing in dissociated Purkinje neurons. *The Journal of neuroscience : the official journal of the Society for Neuroscience*, 23(29):9650–9663, 2003.

[8] Michael D. Forrest. Mathematical Model of Bursting in Dissociated Purkinje Neurons. *PLoS ONE*, 8(8), 2013.

[9] Zayd M Khaliq, Nathan W Gouwens, and Indira M Raman. The contribution of resurgent sodium current to high-frequency firing in Purkinje neurons: an experimental and modeling study. *The Journal of neuroscience : the official journal of the Society for Neuroscience*, 23(12):4899–912, 2003.

[10] A Destexhe, D Contreras, T J Sejnowski, and M Steriade. A Model of Spindle Rhythmicity in the Isolated Thalamic Reticular Nucleus. *Journal of neurophysiology*, 72(2):803–818, 1994.

[11] E D'Angelo, Thierry Nieus, Arianna Maffei, Simona Armano, Paola Rossi, Vanni Taglietti, Andrea Fontana, Giovanni Naldi, and Egidio D Angelo. Theta-frequency bursting and resonance in cerebellar granule cells: experimental evidence and modeling of a slow k+-dependent mechanism. *J Neurosci*, 21(3):759–770, 2001.

[12] W. Akemann. Interaction of Kv3 Potassium Channels and Resurgent Sodium Current Influences the Rate of Spontaneous Firing of Purkinje Neurons. *Journal of Neuroscience*, 26(17):4602–4612, 2006.

[13] Mary Womack and Kamran Khodakhah. Active contribution of dendrites to the tonic and trimodal patterns of activity in cerebellar purkinje neurons. *Journal of Neuroscience*, 22(24):10603–10612, 2002.